

Highly Efficient Ultra-low Loading Pd Supported on MAX Phases for Chemoselective Hydrogenation

Mihaela-Mirela Trandafir, Florentina Neatu, Iuliana M Chirica, Stefan Neatu, Andrei C. Kuncser, Elena I Cucolea, Varun Natu, Michel W Barsoum, and Mihaela Florea

ACS Catal., **Just Accepted Manuscript** • DOI: 10.1021/acscatal.0c00082 • Publication Date (Web): 24 Apr 2020

Downloaded from pubs.acs.org on April 25, 2020

Just Accepted

“Just Accepted” manuscripts have been peer-reviewed and accepted for publication. They are posted online prior to technical editing, formatting for publication and author proofing. The American Chemical Society provides “Just Accepted” as a service to the research community to expedite the dissemination of scientific material as soon as possible after acceptance. “Just Accepted” manuscripts appear in full in PDF format accompanied by an HTML abstract. “Just Accepted” manuscripts have been fully peer reviewed, but should not be considered the official version of record. They are citable by the Digital Object Identifier (DOI®). “Just Accepted” is an optional service offered to authors. Therefore, the “Just Accepted” Web site may not include all articles that will be published in the journal. After a manuscript is technically edited and formatted, it will be removed from the “Just Accepted” Web site and published as an ASAP article. Note that technical editing may introduce minor changes to the manuscript text and/or graphics which could affect content, and all legal disclaimers and ethical guidelines that apply to the journal pertain. ACS cannot be held responsible for errors or consequences arising from the use of information contained in these “Just Accepted” manuscripts.

Highly Efficient Ultra-low Loading Pd Supported on MAX Phases for Chemoselective Hydrogenation

Mihaela M. Trandafir,^{1#} Florentina Neațu,^{1#} Iuliana M. Chirica,^{1,2} Ștefan Neațu,¹ Andrei C. Kuncser,¹ Elena I. Cucolea,³ Varun Natu,⁴ Michel W. Barsoum*⁴ and Mihaela Florea^{1*}

¹National Institute of Materials Physics, 405A Atomistilor Street, 077125 Magurele, Romania

²University of Bucharest, Faculty of Physics, 405 Atomistilor Street, 077125 Magurele, Romania

³Research Center for Instrumental Analysis SCIENT, Petre Ispirescu Street, no. 1, 077167 Tancabesti, Ilfov, Romania

⁴Department of Materials Science and Engineering, Drexel University, Philadelphia, Pennsylvania 19104, USA

authors with equal contribution

ABSTRACT: Palladium is one of the most efficient metals for the hydrogenation of organic compounds. But when molecules, such as nitroaromatics, with several reducible functionalities are hydrogenated, Pd - like any other very active metal such as nickel or platinum - often behaves unselectively. One strategy to render Pd more selective is to choose the proper support. Herein, we show that MAX phase powders of Ti_3SiC_2 , Ti_2AlC or Ti_3AlC_2 can chemoselectively hydrogenate 4-nitrostyrene to 4-aminostyrene, with 100 % selectivity. At around 3-4 %, the conversions, however, are low. To boost the latter, we loaded Ti_3SiC_2 with 0.0005 wt.% Pd and increased the conversion to 100% while maintaining the 4-AS selectivity at > 90%. By optimizing the Pd loading, we were also able to increase the turnover frequency 100-fold relative to previous literature results. The identification of this highly efficient and chemoselective system has broad implications for the design of cost-effective, earth-abundant, non-toxic, metal catalysts, with ultra-low noble metal loadings.

KEYWORDS: MAX phase, 4-nitrostyrene, chemoselective hydrogenation, low noble metal amount, palladium

INTRODUCTION

Reduction with hydrogen, H₂, of only one functional group when several functionalities are present in a molecule is not trivial because the thermodynamic driving forces can be comparable. One way to address this problem has been to use solid catalysts that can chemoselectively orient the desired reactions. A chemoselective catalyst has to distinguish and preferentially interact with one functional group, while avoiding the transformation of the others. There are only few generally applicable catalytic systems for the selective reduction of a nitro group in the presence of C=C, C=O or C≡N groups. Pd is a very efficient metal for the hydrogenation of organic compounds, but is often unselective. Several strategies have been tried, chief amongst them is the proper choice of support, that due to its architecture and interaction with the noble metal increases selectivity. Another approach is to decrease of number of active metal sites by adding additives such as oxides, other metals, etc., but in most cases at the expenses of activity.¹ For instance, to chemoselectively reduce the nitro group via catalytic processes when carbon-carbon double bonds are present in the molecules is considered a big challenge, since functionalized aniline derivatives resulting from hydrogenation of nitro-compounds are key intermediates for a large palette of chemical products with important industrial applications.²⁻⁴

To date, and as far as we are aware, the chemoselectivity to aniline compounds is carried out only in the presence of metals such as Pt, Au, Ru, Ni, Fe, Ag and Rh, as mono or bimetallic catalysts.⁵⁻⁷ The best results are obtained using Au nanoparticles (NPs) deposited on a support, or by using a bimetallic Au-Pt NPs supported on TiO₂.^{8, 9} In particular, recently the hydrogenation of 4-nitrostyrene (4-NS) to 4-aminostyrene (4-AS) has been achieved using colloidal Co-Ru nanoparticles suspensions,¹⁰ Pt supported on a W-TiO₂ modified with organic thiol^{11, 12} or Pd nanosheets suspensions.¹³ However, the development of true heterogeneous catalysts without the use of additives is highly desirable. In a recent review paper, it was shown how chemoselectivity to nitro group reduction can be induced in unselective metals by controlling the architecture of the metal catalysts⁸ and choosing the right support. In spite of all efforts dedicated to this topic over the last few decades, chemoselectivities close to 100 % have remained elusive over true heterogeneous materials.

The MAX phases are ternary early transition metal carbides and/or nitrides with a layered hexagonal crystal structure.^{14, 15} The moniker of these materials derives from their chemical formula, M_{n+1}AX_n, where M is an early transition metal, A is mostly a group 13 or 14 element, X is carbon and/or nitrogen, and n=1, 2, 3 or 4. Most of these phases were discovered in the sixties by Nowotny and co-workers, and lay dormant in the literature until the mid eighties

1
2
3 when they were finally processed in fully, dense and predominantly single phase form which
4 in turn allowed their unusual properties to be documented.¹⁶ The original set numbered around
5 50;¹⁷ today over 150 phases are known to exist, with more being discovered on a routine basis.¹⁸
6
7

8 The MAX phases are unique in a sense that they combine properties of both metals and
9 ceramics. Similar to metals, they are readily machinable, possess high electronic and thermal
10 conductivities. In some cases, the electronic conductivities exceed those of the parent transition
11 metal. They are also damage and thermal shock tolerant.¹⁵ Like ceramics some are lightweight,
12 creep and oxidation resistant and refractory.
13
14
15
16

17 Despite the fact that these phases were rediscovered over two decades ago and thousands
18 of studies on many of their properties have been explored, their use as catalysts had been totally
19 ignored until 2017, when Ng et al. showed the potential of Ti_3AlC_2 – a MAX phase - in selective
20 oxidation reactions.¹⁹ The useful catalytic activity was shown to most likely derived from a
21 very thin, presumably non-stoichiometric, Al and Ti mixed oxide surface layer containing
22 oxygen vacancies.
23
24
25
26

27 To the best of our knowledge, no hydrogenation reactions have been reported so far where
28 a MAX phase was used as either a catalyst or support. Herein, we explore the use of select
29 MAX phases, and more importantly as a support for Pd nanoparticles, NP, at exceedingly low
30 concentrations, for the chemoselective hydrogenation of a functionalized nitro-compound, 4-
31 NS. The product of interest, 4-AS, is an important platform molecule in organic synthesis for
32 a variety of agrochemicals and pharmaceuticals.²
33
34
35
36

37 In this study we report on a new generation of MAX-phase catalysts, in general, and Pd
38 NPs supported on Ti_3SiC_2 in particular, for the selective – in some cases 100 % – hydrogenation
39 of 4-NS to 4-AS with a turnover frequency (TOF) as high as $4.7 \times 10^3 \text{ h}^{-1}$, which represents
40 roughly a 100-fold increase over the most selective catalyst reported to date in the literature
41 (See Figure 1a and Table S1). To also probe the generality of our approach we performed
42 catalytic hydrogenation on other molecules containing multiple functional groups, such as 3-
43 nitrostyrene (3-NS) and cinnamaldehyde. Additionally, a few runs were carried out where the
44 MAX-phase was used as support for Ni.
45
46
47
48
49
50
51
52
53
54
55
56
57
58
59
60

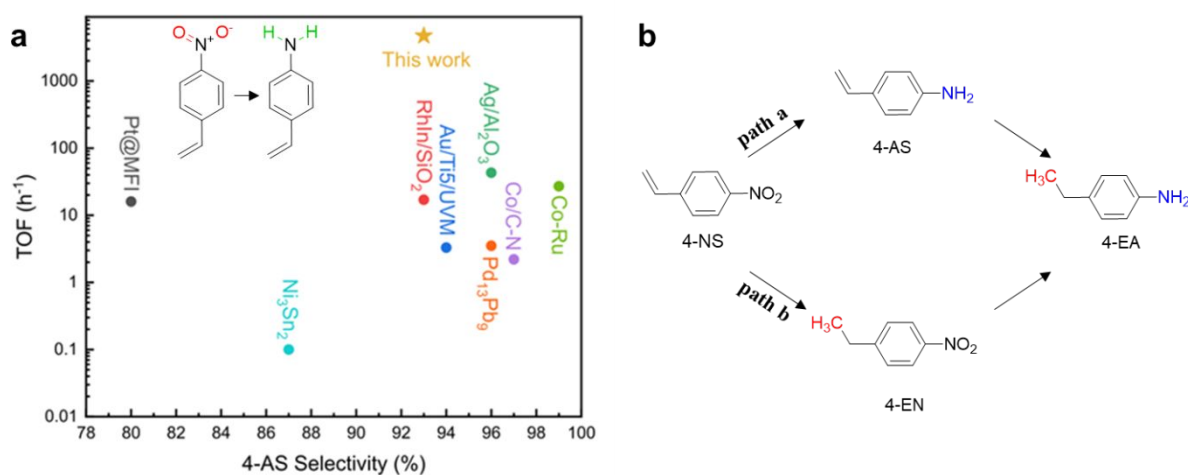


Figure 1: a) Semi-log plot of our TOF results compared with some of the highest reported in the literature for catalysts with 100% conversion and > 80% selectivities of 4-NS to 4-AS. Left top inset shows 4-NS molecule; top right inset shows desired molecule, 4-AS. b) Reaction pathways for hydrogenation of 4-NS.

RESULTS AND DISCUSSION

Catalytic activity of the MAX phases. The MAX phases were prepared by heating elemental powders in a tube furnace under flowing argon, Ar, at 1500 °C for 3 h. X-ray diffraction showed that in all cases the resulting powders were predominantly single-phase. Three phases were synthesized: Ti₃SiC₂, Ti₃AlC₂ and Ti₂AlC. The XRD patterns of the Ti₃SiC₂ powders is shown in Figure S1. Not surprisingly, given the ultra-low loading of Pd used herein, impregnating these powders with Pd does not change the XRD patterns in any way (Figure S1).

The chemoselective hydrogenation of 4-NS was performed in the presence of the MAX phase using heptane as a solvent and hydrogen, H₂ gas, as a reducing agent. The reaction was performed at different temperatures, H₂ pressures and reaction times. The reaction products identified were 4-AS, 4-ethylnitrobenzene (4-EN) and 4-ethylaniline (4-EA) (see Figure 1b and Figure S2). Blank tests, in the absence of the catalyst, were also performed and no conversion of 4-NS was evidenced. Moreover, the carbon balance was always close to 100%, indicating that no side reactions occurred.

Regardless of the MAX composition powders used, as shown in the top entries in Table 1, we successfully hydrogenated 4-NS, with 100 % selectivity, into the product of interest, viz. 4-AS. This 100 % selectivity is reported for a MAX phase here for the first time. Similar behavior was also reported for noble metal-free materials, such as graphene, which is able to

hydrogenate acetylenes,²⁰ due to the frustrated Lewis pairs or defects present in the material which are able to heterolytically activate H₂.²¹

The low conversions can be, at least partially, explained by the fact that the MAX phases have a low H₂ dissociation rate as evidenced by H₂-TPD experiments that showed that not only were very small amounts of H₂ adsorbed on the MAX phase surfaces but that they also desorbed at temperatures < 100 °C (Figure S3). Since the H₂ activation usually takes place readily on metals, it is reasonable to suppose that the presence of a thin native oxide layer – present here - on the MAX phases' surfaces is responsible for the low adsorptions.

Increasing the H₂ pressure from 1.1 to 2.5 MPa increased the conversions slightly for all samples (see entries 1-6 in Table 1), but they remained low, around 4%. Note that the selectivity remained at ≈ 100% for Ti₂AlC and Ti₃SiC₂ (entries 4 and 6 in Table 1). The high selectivity to aniline is probably due to the preferential adsorption of nitro groups over C=C bonds on the Ti containing support, such as TiO₂, as demonstrated in previous reports,⁸ or due to the defects present in MAX phases,¹⁸ which might heterolytically dissociate H₂, thus hydrogenating preferentially the polar group (nitro) found in 4-NS.²²

Table 1. Catalytic performance of MAX phases-based catalysts for 4-NS conversion

Entry	Catalyst	H ₂ pressure (MPa)	Conversion (%)	Selectivity (%)		
				4-AS	4-EN	4-EA
1	Ti ₂ AlC	1.1	< 1	100	-	-
2	Ti ₃ AlC ₂	1.1	< 1	100	-	-
3	Ti ₃ SiC ₂	1.1	< 1	100	-	-
4	Ti ₂ AlC	2.5	1	100	0	0
5	Ti ₃ AlC ₂	2.5	4	13	87	0
6	Ti ₃ SiC ₂	2.5	3	100	0	0
7	TiC	2.5	6	51	49	-
8	MXene	2.5	0	-	-	-

Reaction conditions: 0.0134 mmol substrate; 4 mg catalyst; 3 mL of heptane; 24 h, 140 °C, 2.5 MPa H₂

To prove this, additional experiments were performed on bulk TiC (Alfa Aesar) and on the corresponding MXene, Ti₃C₂T_z. The conversion of the TiC powders at ≈ 6% was comparable to that of the MAX phases. At 51%, however, the selectivity was roughly half that of the MAX phases (Table 1, entry 7). In the case of MXene no conversion was obtained (Table 1, entry 8).

Based on these results it was concluded, not unreasonably, that H₂ dissociation was the rate limiting step. If that were the case, then we conjectured that the presence of a metal capable of activating H₂ should increase our conversions. This is why we impregnated Ti₃SiC₂ with Pd.

Catalytic activity of Pd/MAX phases. The next challenge was to find the optimal Pd quantity necessary, while maintaining a selectivity to 4-AS of close to 100%. To that effect the

following very low Pd loadings were tested: 0.05 wt.% and 0.0005 wt.%. The catalytic results are summarized in Table 2.

Table 2. Catalytic performance of Pd/MAX phases catalysts, prepared by different methods for 4-NS conversion

Entry	Catalyst	Pd loading (ICP-MS) (wt.%)	Conv. (%)	Selectivity (%)			TOF (ICP) (h ⁻¹)
				4-AS	4-EN	4-EA	
1	0.05 wt.% Pd/Ti ₃ SiC ₂	0.01060‡	100	0	47	53	1.4*10 ²
2	0.0005 wt.% Pd/Ti ₃ SiC ₂	0.00033‡	100	0	68	32	1.1*10 ³
3	0.0005 wt.% Pd/Ti ₃ SiC ₂ _DP	0.00014‡	100	25	0	75	4.7*10 ³

The addition of 0.05 wt.% or 0.0005 wt.% of Pd to Ti₃SiC₂ by impregnation increased the conversion to 100%, but the process was no longer selective (Table 2, entries 1 and 2). The advanced hydrogenation product, 4-EA was obtained via the formation of 4-EN (path b in Figure 1b).

To broaden the scope of Pd loading, we changed the Pd supporting method, from impregnation to deposition-precipitation (DP). Doing so improved the chemoselectivity to 4-AS, while maintaining the total conversion of 4-NS. A selectivity of 25% for 4-AS and 75% for 4-EA was thus obtained (Table 2, entry 3).

The ICP-MS analysis performed for the three catalysts (Table 2) demonstrated that changing the technique also diminished the Pd content and the amount of Pd found in the catalyst prepared by DP was three times lower than in the case of the impregnation method (see Table 2, entry 3). Such behavior was expected, since the DP technique supposes free adsorption of Pd onto the support from a higher volume solution and crucially also includes a washing step, while impregnation has the advantage of using smaller volumes that enable the deposition of higher Pd amounts onto the support and no washing step is needed. This is supported by XPS analysis (Figure S4), in which the Pd was evidenced on the surface for the sample prepared by impregnation, but not the surface prepared by the DP technique. For the latter, the Pd was below the detection limits of our XPS (see Figure S4e).

It is important at this point to note that the deposition of Pd by the two methods chosen here do not modify the MAX phase structure in any way (see Figures S1, S4). TEM images confirmed that all the observed samples showed similar morphology and structure (thin sheets of Ti₃SiC₂ (Figure 2). No changes in the MAX powders after impregnation, within TEM resolution, were observed. X-ray mappings performed with a nm sized probe showed metallic Pd nanocrystals with a size in the 10 nm range in the case of 0.05 wt.% Pd doped sample

(Figure 3). In all other cases, no clear evidence in the TEM for Pd was found, most probably because of its very low concentrations in the samples.

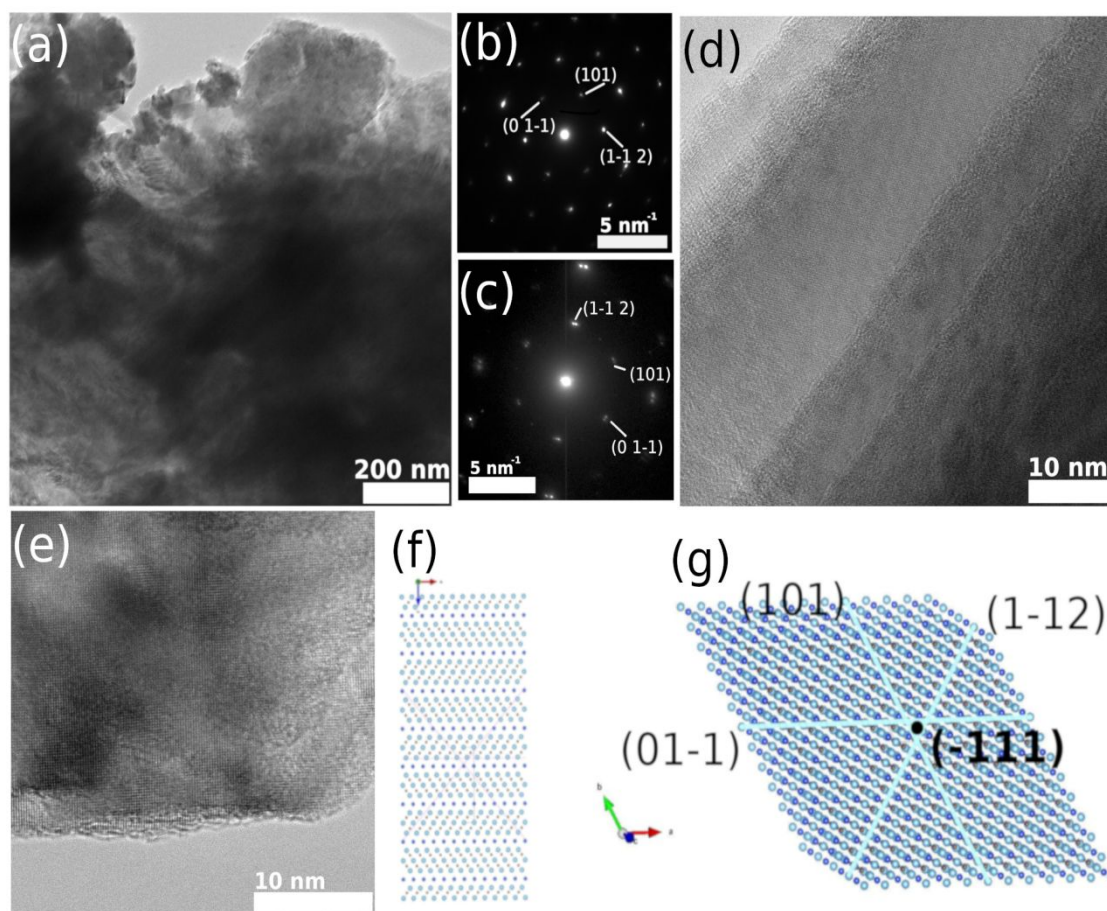


Figure 2: HRTEM images for Ti_3SiC_2 . Powdered sample has been observed generally as sheets of Ti_3SiC_2 which tend to be in the same orientation. Results in (a)-(d) have been provided in the $g = (-111)$ zone axis orientation. Image (e) shows a thin sheet observed along c-axis as identified by high resolution imaging. (f) Visualization for electronic and structural analysis (VESTA) structural model of Ti_3SiC_2 on c zone axis perspective. (g) VESTA structural model showing main lattice planes of Ti_3SiC_2 identified in electron diffraction patterns.

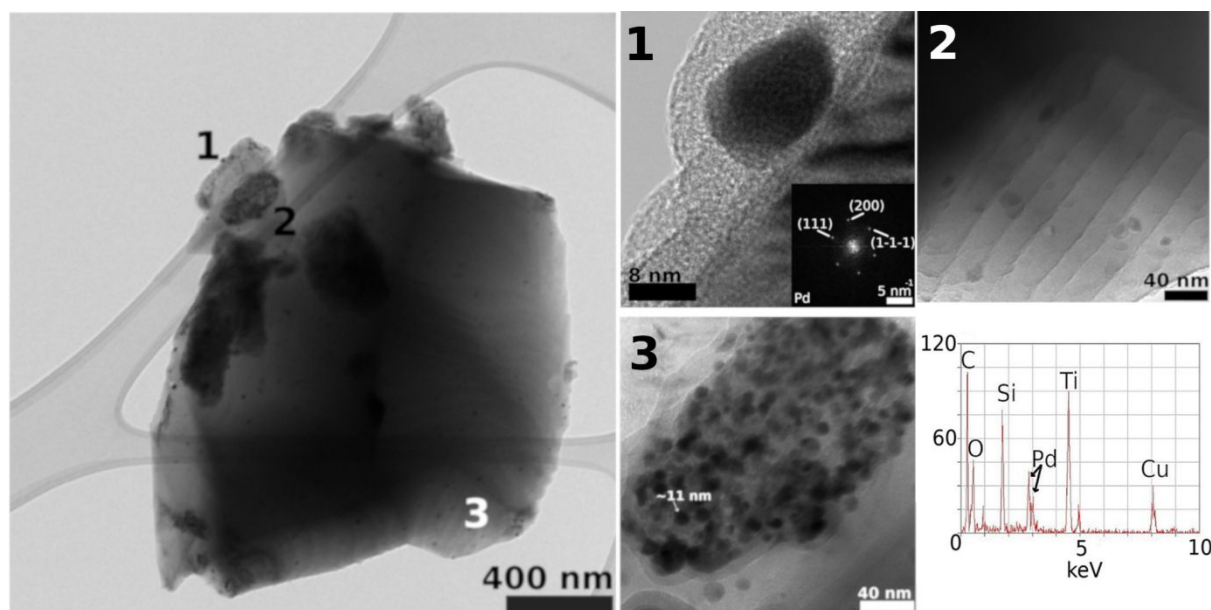


Figure 3: Large area TEM image of 0.05% Pd/Ti₃SiC₂ showing numbered regions of interest (ROI) 1 to 3. HRTEM image of Pd NP with Selected Area Diffraction inset on ROI 1 (Figure 3.1), image of Pd NPs cluster and attached X-ray spectra showing Pd peak on ROI 2 (Figure 3.2) and a high magnification image on the ROI 3 of Pd/Ti₃SiC₂ sheet (Figure 3.3) X-ray maps performed with a nm sized probe showed metallic Pd nanocrystals with a size in the 10 nm range in the case of the 0.05 wt.% Pd doped sample.

With the purpose of preserving the preferential selectivity obtained on Ti₃SiC₂ and to better control the amount of Pd, a third strategy was employed, viz. mechanically mixing Ti₃SiC₂ powders with those that were impregnated with Pd (viz. Pd/Ti₃SiC₂ catalyst). The schematic preparation of mechanical mixture is depicted in Scheme 1 and described in the experimental section. The exact compositions of the mixtures are listed in Table S2 and the results are listed Table 3, entries 1-9.



Scheme 1. Schematic of mechanical mixture preparation and its benefits.

Table 3. Catalytic performance of Pd/MAX phases catalysts (mechanically mixed) for 4-NS conversion

Entry	Catalyst	Pd loading (ICP-MS) (wt.%)	Conv. (%)	Selectivity (%)			TOF (ICP) (h ⁻¹)
				4-AS	4-EN	4-EA	
1	Pd/Ti ₃ SiC ₂ _mix1	0.00002 ^a	4	100	0	0	3.6*10 ³
2	Pd/Ti ₃ SiC ₂ _mix2, cycle 1	0.00013 ^a	59	73	19	8	2.8*10 ³
3	Pd/Ti₃SiC₂_mix2, cycle 2	0.00013^a	100	93	0	7	4.7*10³
4	Pd/Ti ₃ SiC ₂ _mix3	0.00022 ^a	100	58	0	42	2.8*10 ³
5	Pd/Ti ₃ SiC ₂ _mix4	0.00254 ^a	100	10	0	90	4.7*10 ²
6	Pd/TiC_mix2, cycle 1	nd	100	-	97	3	nd
7	Pd/TiC_mix2, cycle 2	nd	18	-	100	-	nd
8	Pd/Ti ₂ AlC_mix2	nd	52	27	73	0	nd
9	Pd/Ti ₃ AlC ₂ _mix2	nd	100	-	99	1	nd
10	Pd/Ti ₃ C ₂ T _z _mix2, cycle 1	nd	90	-	95	5	nd
11	Pd/Ti ₃ C ₂ T _z _mix2, cycle 2	nd	25	-	100	-	nd

Nd = not determined

The mechanically mixed Pd/Ti₃SiC₂_mix1 had the same catalytic behavior as Ti₃SiC₂ without Pd (Table 3, entry 1). The reason is mostly probably the almost negligible (0.00002 wt.%) amount of Pd. By slightly increasing the Pd amount to 0.00013 wt.%, the selectivity was 73% 4-AS and the conversion was 59% (Table 3, entry 2). Interestingly, after the second reaction cycle of this sample, the catalytic performance improved, and the selectivity to 4-AS reached 93%, at a conversion of 100% (Table 3, entry 3).

To test whether the “boomerang effect” was applicable here we carried out hot filtration experiments. However, since the results before and after hot filtration were identical, we conclude that the well-known “boomerang effect”^{23, 24} is not responsible for the induction period observed herein. We also checked the similarity with the Lindlar catalyst, for which the selectivity is improved by protecting the highly active metals sites with other elements and organic or inorganic compounds.²⁵ In our case, we added small amounts of 4-AS and 4-EN in the initial reaction mixture (Table S3, entries 1 and 2) and found that the conversion and chemoselectivity decrease. These results suggest that our catalytic system does not behave like Lindlar catalyst.²⁶

The good results obtained after the second reaction cycle are thus most probably caused by an induction period, that reflects the time needed for the promotion of a strong metal–support interaction which is often invoked to be critical in catalysis.²⁷ Also, there are different possible explanations for the improvement of the chemoselectivity, not evidenced experimentally by us, but sustained theoretically²⁸ and experimentally²⁹ by other studies: i) through electronic effects,

1
2
3 Pd transforms into a more stable adsorption structure and a complex interplay of the electronic
4 interactions between the adsorbate molecules and the metal surface which can lead to changes
5 in the mechanism of H₂ activation²⁸ and/or ii) through geometric effects, the *in situ* reduction
6 of the Pd cluster size leading to a decreased number of adjacent adsorption sites.³⁰ These
7 comments notwithstanding, more work is needed to better understand what is occurring as a
8 function of time/cycling of our system.
9

10
11
12
13 Further increasing the Pd content (Table 3, entries 4 and 5) improves the catalytic
14 conversion, but the selectivity to 4-AS decreases to 58% and 10%, respectively. Apparently,
15 the Pd/Ti₃SiC₂_mix2 sample possesses the optimal Pd amount necessary to reach a conversion
16 of 100%, while maintaining the MAX phases' selectivity to 4-AS at > 90%.
17
18
19

20
21 By assuming that all the Pd atoms were accessible to the reactants, we estimated the total
22 number of 4-NS moles transformed by moles of Pd per time, TOF, of all tested catalysts. The
23 TOF values for 4-NS hydrogenation varied from 10² to 10³ h⁻¹ (last column in Table 2 and 3).
24 These values are exceptionally high especially compared with literature data (see Table S1 and
25 Figure 1a). For the latter, we only report systems for which the selectivity was > 80%.
26
27
28

29 **Catalyst recyclability and stability.** Since, the catalytic stability is crucial in catalytic
30 processes, we tested the stability of Pd/Ti₃SiC₂_mix2 sample over 6 consecutive cycles. From
31 the results (Figure 4) it is obvious that our system is stable for at five reaction cycles.
32 Deactivation starts only during the sixth reaction cycle. A possible reason for the 20%
33 deactivation in the 6th cycle might be the partial blockage of the active centers with reaction
34 products, as evidenced by ATR-FTIR spectroscopy and XPS (Figures S5 and S6). Moreover,
35 the results of the leaching tests (compare entries 3 and 4 in Table S3) showed that 4-NS
36 hydrogenation stops when the catalyst is removed from the reaction media, indicating that no
37 Pd was solubilized in the reaction mixture and thus no homogenous reactions can occur. The
38 hot filtration experiments also indicate that Pd does not leach from the catalyst surface.
39
40
41
42
43
44
45
46
47
48
49
50
51
52
53
54
55
56
57
58
59
60

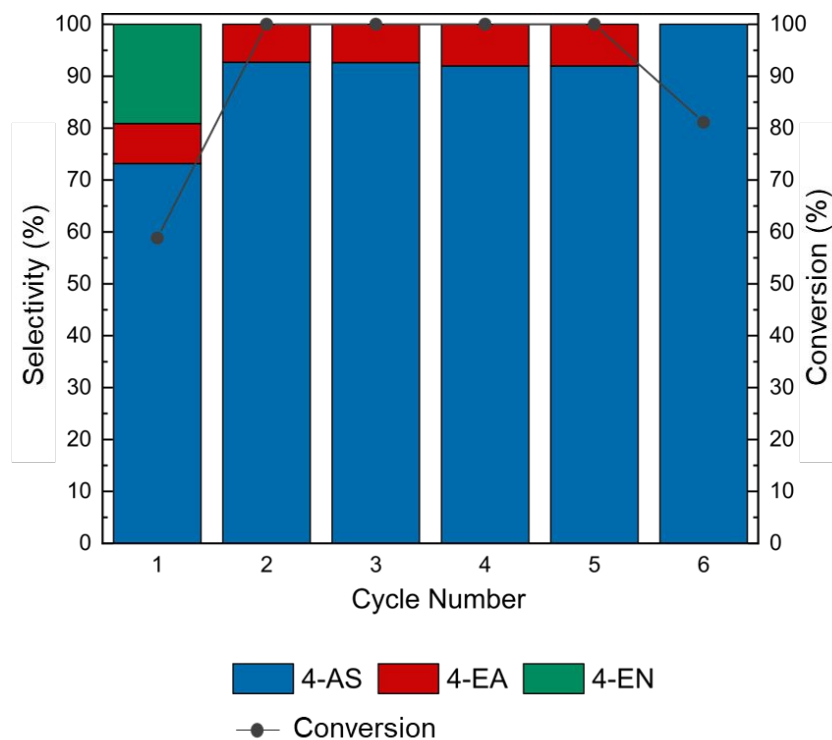


Figure 4: Stability tests performed on Pd/Ti₃SiC₂_mix2 as catalyst for 4-NS hydrogenation, as a function of cycle number.

It is also crucial to note that phenyl hydroxylamine, which is commonly obtained during 4-NS hydrogenation reactions performed on oxide surfaces,^{8, 11} was not detected. As this compound is a powerful explosive, its absence is necessary, and desirable, in industrial applications/settings. Our results bode well for the use of this system commercially.

Catalytic activity on other substrates. To explore the general utility of our optimized catalyst - Pd/Ti₃SiC₂_mix2 – we attempted to hydrogenate 3-NS to 3-AS. The results (Table S4, entry 1) show that 100% conversion is possible with a selectivity of 96% after the first reaction cycle. Here again, unprecedented TOF values that are ≈ 100 fold higher than those reported so far in the literature are obtained.^{6, 8, 31} Changing the position of functional groups from para- to meta- on the aromatic ring improve the substrate conversion (see Table S4, entries 1, 2 and 4, 5) and also the selectivity. The electronic effects of the reactants could influence the catalytic performance; similar results were observed on Ru based catalyst.³² Very interesting results converting 4- or 3-nitrobenzaldehyde in the presence of our catalytic system were obtained, i.e. reductive N-alkylation of nitrobenzaldehyde in one step, with a very high chemoselectivity to the alkyl-derivative (96%), which proceed only after reduction of nitro-group (see Table S4, entries 4 and 5).³³ Several others nitro-olefins were tested and we

1
2
3 identified that Pd/Ti₃SiC₂_mix2 was able to chemoselectively (83%) hydrogenate 4-
4 nitrophenol (Table S4, entry 6).

5
6 Corma et al.⁶ tested 5% Pd/C, among others, as catalyst in the hydrogenation of several
7 substituted nitro-compounds. It was shown that aliphatic molecules, such as 1-nitro-
8 1cyclohexene, are more difficult to be hydrogenated compared with aromatic nitro compounds.
9 It was also our case for other types of molecules containing C=C and nitro substituents as can
10 be observed in Table S4, entries 3, 7 and 8. The presence and/or the nature of the second
11 functional group influences the activity and the selectivity of the catalytic system and attention
12 must be paid to the type of solvent used or reaction temperature.

13
14 We also tested optimized catalysts for the hydrogenation of cinnamaldehyde to
15 hydrocinnamaldehyde and/or cinnamyl alcohol (Table S4, entry 9). Our catalyst
16 chemoselectively hydrogenated cinnamaldehyde to hydrocinnamaldehyde with 80%
17 selectivity and 94% conversion. The TOF's were comparable with data presented in literature.³⁴
18 In accordance with the literature,³⁵ Pd deposited on different supports reacts much faster with
19 C=C bonds than with C=O bonds and this could explain why the selectivity to cinnamyl alcohol
20 is only 3%.

21
22 Overall, however, our results, obtained in conditions not yet optimized, reveal the *potential*
23 of Pd/MAX phase materials as chemoselective catalyst for nitro group hydrogenation.

24
25 When Pd is replaced by Ni, another nonselective hydrogenation metal, using as support the
26 most selective MAX powder, Ti₃SiC₂, the selectivity to 4-AS remained at 100% (Table S3,
27 entry 5). However, the conversions were around 1% most probably because the amount and
28 type of Ni and its oxidation state were not optimal for this reaction. It is reasonable to assume
29 here that, like for Pd, an optimum Ni loading also exists. This study is ongoing.

30 31 ***General assessments on the chemoselective hydrogenation behavior of Pd/MAX phase***

32
33 The development of active and selective catalysts represents a crucial point in
34 chemoselective hydrogenations, and in this context beside the composition of a catalyst the
35 preparation method also has an influence over the reaction's conversion/selectivity. Indeed, if
36 one compares catalysts with almost the same amount of Pd (~0.00014 wt.% by ICP-MS)
37 prepared by impregnation (Table 3, entry 2) and DP (Table 2, entry 3), the conversion increases
38 from 59% to 100% when using the catalyst prepared by impregnation vs. the DP method. TEM
39 investigations show Pd clusters formation for 0.05 wt.% Pd/Ti₃SiC₂ prepared by impregnation
40 (used in the mix samples), while for DP we assume, based on literature data,³⁶ that the metal
41 loading is better dispersed (no clear evidence in TEM, due to technical limitations). Therefore,
42
43
44
45
46
47
48
49
50
51
52
53
54
55
56
57
58
59
60

1
2
3 even though the Pd amount is comparable in both catalysts, the number of accessible sites
4 appears to be a function of the preparation method. Thus, by DP a good dispersion is obtained
5 leading to a higher number of accessible active sites and total conversion, while through
6 impregnation, larger clusters are formed limiting the number of accessible sites and
7 consequently the conversion (59 %).
8
9

10
11 Usually, the improvement of the selectivity is accompanied by a decrease of catalytic
12 activity.³⁷ Indeed, the results depicted in Table 3 (entries 1, 2, 4 and 5) underline the critical
13 importance of Pd content/dispersion onto a selective support and that exceeding an optimal Pd
14 value results in masking the selective effect of Ti_3SiC_2 , leaving in place only a non-selective
15 Pd effect. For samples with the same degree of conversion (100%), large Pd clusters, from
16 impregnated sample for instance, transform unselectively 4-NS (Table 2, entry 2), while small
17 Pd particles, very well dispersed obtained by the DP method, produces 4-AS and 4-EA (Table
18 2, entry 3). Similar behaviour was observed for other different metal-support catalysts used in
19 the hydrogenation of 4-NS, when big metal clusters are formed during preparation the
20 selectivity diminishes.^{1, 38} This observation can be ascribed to the different ways of adsorption
21 and activation of H_2 . It is well known that H_2 activation constitutes a critical step in
22 chemoselective hydrogenation reactions, and moreover, that homolytic activation of H_2 is
23 promoted by larger metal particles, is which are not selective.³⁹
24
25

26
27 In contradistinction, a higher metal dispersion to single atoms heterolytically cleave the H_2
28 molecule into H^+/H^- pairs, which are more prone to hydrogenate the polar groups rather the
29 non-polar ones.³⁷ The heterolytic cleavage of H_2 into H^+/H^- pairs on Pd/support catalysts occurs
30 in a similar way as in the Shvo–Noyori catalysts and frustrated Lewis pairs, where the support
31 serves as a proton acceptor, while the Pd atom as the hydride acceptor.³⁷
32
33

34
35 Our strategy to better control the Pd dispersion, by using mechanical mixing, led to a
36 selectivity of 73% (Table 3, entry 2) for an ultra-low amount of Pd (130 ppm). In this context,
37 we cannot exclude the generation of “single atom catalyst” that might occur, that could in turn
38 heterolytically activate H_2 , which has been demonstrated to be very effective for
39 chemoselective hydrogenations.³⁷ Furthermore, Perez *et al.* using DFT calculations
40 demonstrate that atomically dispersed Pd atoms lead to high activity and selectivity due to a
41 facile hydrogen activation and reactant adsorption on these types of sites.⁴⁰
42
43

44
45 As presented in Tables 1 and 3, the composition of the support, its surface and, most
46 probably, the metal-support interaction play an important role in this reaction. In comparison
47 with Ti_3SiC_2 , TiC and $\text{Ti}_3\text{C}_2\text{Tz}$ show a different behavior in hydrogenation of 4-NS when Pd
48 was deposited by the same method on its surface (see Table 3, entries 6 and 10) for 100% and
49
50
51
52
53
54
55
56
57
58
59
60

90% conversion of 4-NS, respectively, crucially *no* 4-AS formed. The induction period was also checked for these materials and instead of an improvement as in the case of Ti_3SiC_2 a deactivation occurred; in the second cycle the conversion diminished drastically to 18% and 25% (Table 3, entries 7, 11) respectively, most probably due to a lower metal-support interaction. These results alone imply that oxides formed during aerobic oxidation on the MAX surfaces are responsible for the catalysis; no other interpretations are plausible.

To gain more information Raman spectroscopy was performed on Ti_3SiC_2 and TiC. The spectra depicted in Figure 5 revealed the four characteristic Raman active modes of $2E_{2g}$, E_{1g} and A_{1g} at 167 cm^{-1} , 223 cm^{-1} , 272 cm^{-1} and 358 cm^{-1} , named ω_1 , ω_2 , ω_3 , ω_4 , related to C–Ti–Si bonds for Ti_3SiC_2 . These vibrations are comparable with those previously reported by some of us.⁴¹ The vibration modes from 609 and 670 cm^{-1} are related to the C–Ti–C bonds. Crucially, a supplementary Raman mode at 128 cm^{-1} , which correspond to $\alpha\text{-SiO}_2$ was observed in the ternary MAX phase.⁴² The presence of SiO_2 in the native oxide is not too surprising because when Ti_3SiC_2 is oxidized at high temperatures, a duplex rutile and SiO_2 scale forms.⁴³ We conjecture at this time that it is the presence of SiO_2 that may help orient the 4-NS at the surface of the support. A similar improved selectivity to 4-AS was also observed for other titanium-modified SiO_2 on which Pd was deposited.⁴⁴ As already emphasized by Boronat et al.⁷ the repulsion between the electrons from the aromatic ring and the oxygen electrons from the SiO_2 orient the 4-NS perpendicularly to the surface, while the two oxygen atoms of the nitro group bond to the Ti and Pd surface atoms.

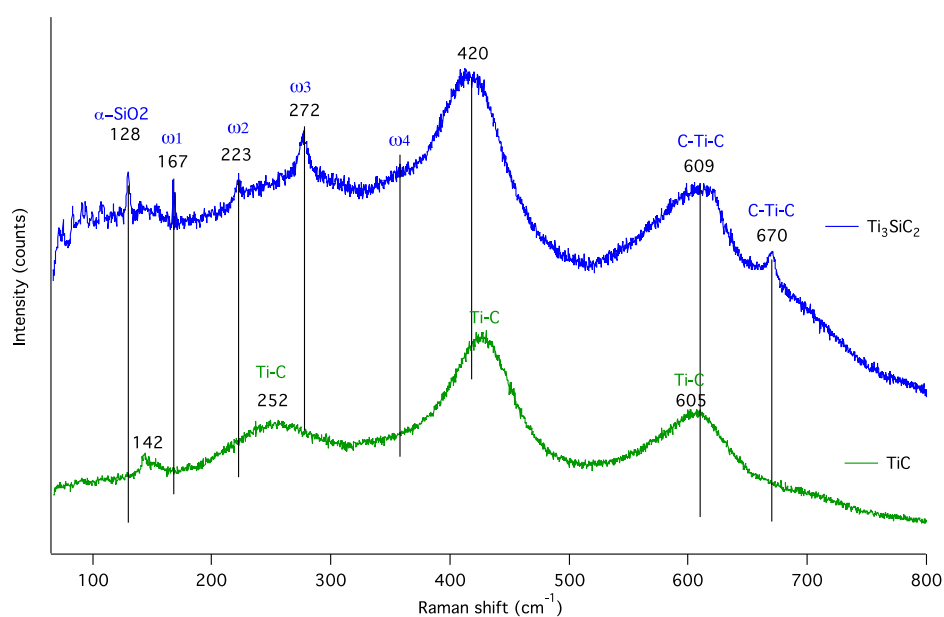


Figure 5: Raman spectroscopy of Ti_3SiC_2 and TiC.

1
2
3
4
5 The same 4-NS hydrogenation was also performed on Pd supported on Ti_2AlC and Ti_3AlC_2
6 MAX phase powders. In this case the selectivity to 4-AS, was much reduced (Table 3, entries
7 8 and 9). Interestingly the selectivity to 4-EN was close to a 100% with a conversion of 100%
8 in the Pd/ Ti_3AlC_2 _mix2 case (Table 3, entry 9). Currently, we know that the oxides that form
9 on Ti_3SiC_2 surfaces (TiO_2 and SiO_2)⁴³ are different than those that form on Ti_3AlC_2 (solid
10 solution between TiO_2 and Al_2O_3),¹⁹ which probably lacks the ability to orient preferentially
11 the 4-NS to form 4-AS.
12
13
14
15
16

17 Finally, it is reasonable to conclude that the high chemoselectivity of the Pd/MAX phase
18 catalyst can be attributed to the synergetic effect between the Pd nanoparticle size and
19 dispersion and the non-Ti containing oxides formed on the MAX phases that preferentially
20 activate the nitro group. If the Ti-containing oxides were solely responsible, then TiC should
21 have worked as well as the MAX phases, which is not observed.
22
23
24
25

26 Lastly, it is important to note that the results obtained herein are a strong function of the
27 nature and thicknesses of the native oxides that form on the MAX phases. This was made clear
28 to us when a second batch of Ti_3SiC_2 powders, nominally synthesized in exactly the same way
29 as the first, were found to have slightly different catalytic properties. Most probably the amount
30 of SiO_2 formed on the surface is different and therefore the second batch behaved more like
31 TiC. We are currently trying to understand what is occurring. This observation brings up a
32 related important question - the answer of which is beyond the scope of this work – viz. what
33 is the relationship between the catalytic activity and the nature of the oxides that form on the
34 different MAX phases? How the nature of these oxides changes during catalysis is also an
35 important topic that we are currently exploring.
36
37
38
39
40
41
42
43
44

45 CONCLUSIONS

46 In conclusion, herein we show that the MAX phases Ti_3SiC_2 , Ti_3AlC_2 and Ti_2AlC are
47 selective in converting 4-NS to 4-AS, but the conversions are low. By using ultra-low amounts
48 of Pd, we were able to maintain the very high selectivity and concomitantly increase the
49 conversion due to the heterolytic activation of H_2 and/or generation of single atom active
50 catalyst. With an optimal loading of very well dispersed 130 ppm Pd, we obtained a conversion
51 of 100% with a selectivity of 93% of 4-NS to 4-AS; higher Pd loadings result in a loss of
52 selectivity. The main role of the Pd is to dissociate/activate the H_2 gas. And while Pd is not an
53 earth abundant element, the very small amounts needed together with the earth abundant and
54
55
56
57
58
59
60

1
2
3 non-toxic nature of the elements in the MAX phases considered here suggests that the cost of
4 raw materials and/or toxicity should not be barriers to potential commercialization.

5
6 These reactions represent the first examples where select MAX phases, with ultra-low
7 amounts of Pd, can be used as catalyst in chemoselective hydrogenation reactions. Thus, this
8 could well be the starting point for designing of a new generation of chemoselective catalysts
9 in the hydrogenation of functionalized nitroderivatives, where the catalytic properties of the
10 MAX phases can be exploited.
11
12
13
14

15 16 17 **METHODS**

18 *Synthesis of MAX phase powders*

19
20 The powders used for this work were: TiC, (Alfa Aesar, 99.5% 2 μm), silicon (Alfa Aesar,
21 99.5%, - 325 mesh), Ti (Alfa Aesar, 99.5%, - 325 mesh) and Al (Alfa Aesar, 99.5%, - 325
22 mesh).
23
24

25
26 The Ti_3SiC_2 powders were made by mixing TiC, Si and Ti powders in a molar ratio of
27 2:1:1, respectively. The mixed powders were ball milled for 24 h at 70 rpm using zirconia balls.
28 The powders were then placed in an alumina tube furnace and heated under flowing Ar at
29 1500°C for 3 h. The heating and cooling rates were set at 5°C min⁻¹. The resulting porous
30 blocks were ground to a powder using a drill press. The milled powders were passed through
31 a 400 mesh (particle size < 38 μm) sieve for further experiments.
32
33

34
35 The same procedure was used to make Ti_3AlC_2 and Ti_2AlC powders. In this case the
36 TiC:Al:Ti ratios used were 2:1.05:1 and 1:1.1:1, respectively.
37
38
39

40 41 **Catalyst synthesis**

42
43 Three methods were used to support Pd on Ti_3SiC_2 .

44 *i) Wet Impregnation Method*

45
46 Pd was supported on Ti_3SiC_2 by a wet impregnation method. The required amount of the
47 Pd precursor (Pd (II) acetate) was dissolved in methanol and the MAX powder was then added.
48 The system was stirred at 40 °C for 16 h, before drying the mixture at 60 °C, under vacuum
49 (10^{-4} MPa), for 5 h.
50
51

52
53 In convert the acetate to Pd supported on the MAX powders, the dried mixture was annealed
54 in a 10 mL min⁻¹ flow of 5 vol % H_2 in Ar at 200 °C at a heating rate 10 °C min⁻¹ for 3 h. The
55 catalyst was collected after cooling to RT and subsequent gradual exposure to air. Materials
56 containing several Pd loadings (0.0005 wt. % and 0.05 wt. %) were prepared. The catalysts in
57 this case are henceforth referred to as 0.0005% Pd/ Ti_3SiC_2 and 0.05% Pd/ Ti_3SiC_2 , respectively.
58
59
60

1
2
3 Palladium (0.05 wt. %) was impregnated on other two MAX phases - Ti_2AlC and Ti_3AlC_2
4 - employing the same procedure as for the 0.05 wt. % Pd/ Ti_3SiC_2 powders.
5
6

7 A 0.05 wt. % Ni/ Ti_3SiC_2 was also prepared also using wet impregnation method,
8 starting from Ni(II) nitrate hexahydrate as precursor. The final material was annealed in 5 vol
9 % H_2 in Ar flow (10 mL min^{-1}) at $450 \text{ }^\circ\text{C}$ at a heating rate $10 \text{ }^\circ\text{C min}^{-1}$, for 3 h.
10
11
12

13 *ii) Deposition-Precipitation Method*

14
15 Palladium was also supported on Ti_3SiC_2 using a deposition-precipitation method, for a
16 calculated concentration of 0.0005 wt. % Pd. The required amount of Pd (II) acetate was
17 dissolved in 5 mL of methanol and the MAX powder was added to the mixture. A 25% NH_4OH
18 solution was then added, drop wise, until a pH 9 was reached at which time the mixture was
19 stirred at $40 \text{ }^\circ\text{C}$ for 16 h. The material was thoroughly washed with distilled water and the
20 material was dried, at $60 \text{ }^\circ\text{C}$, under vacuum, for 5 h. The obtained supported Pd precursor was
21 reduced in a 10 mL min^{-1} flow of 5 vol % H_2 in Ar at $200 \text{ }^\circ\text{C}$ using a heating rate $10 \text{ }^\circ\text{C min}^{-1}$
22 for 3 h. The catalyst was collected after cooling to RT and slowly exposed to air. The final
23 material will henceforth be referred to as 0.0005% Pd/ Ti_3SiC_2 _DP.
24
25
26
27
28
29
30
31

32 *iii) Mechanical Mixing*

33
34 The Pd content of the 0.05 wt. % impregnated catalyst powders was further diluted by hand
35 mixing 0.05%Pd Ti_3SiC_2 powders with extra pure Ti_3SiC_2 powders, in the ratios listed in Table
36 S2. These samples were denoted Pd/ Ti_3SiC_2 _mix1, Pd/ Ti_3SiC_2 _mix2, Pd/ Ti_3SiC_2 _mix3 and
37 Pd/ Ti_3SiC_2 _mix4. Their composition and calculated percentage of Pd, based on our ICP-MS
38 results are also listed in Table S2. For the most part the Pd content measured by ICP described
39 further.
40
41
42
43
44

45 The same procedure was employed for the preparation of Pd/ Ti_2AlC _mix2 and
46 Pd/ Ti_3AlC_2 _mix2 with the proportions listed in Table S2.
47
48
49

50 **Catalytic tests**

51 The catalytic runs were performed in a 20 mL stainless steel autoclave, equipped with a
52 magnetic stirrer. In a typical experiment, the autoclave was loaded with 4 mg of catalyst, 0.0134
53 mmol of substrate and 3 mL of solvent (heptane).
54
55

56 The autoclave was purged 3 times with H_2 in order to remove any residual air and then
57 pressurized with hydrogen to 2.5 MPa. The reaction was carried out at $140 \text{ }^\circ\text{C}$ for different
58 times. At the end of the reaction, the autoclave was cooled down to RT and the H_2 pressure
59
60

1
2
3 was slowly released. The catalyst was separated from the reaction media and the products from
4 the liquid phase were analyzed by GC-MS. Data reproducibility was checked by performing
5 each experiment in duplicate. The obtained results were within $\pm 5\%$ of each other.
6
7
8
9

10 **Stability tests**

11 The stability test was carried out for 4-NS hydrogenation (0.0134 mmol) in the presence of
12 Pd/Ti₃SiC₂_mix2 catalyst (4 mg), using heptane as solvent (3 mL), at 140 °C, 2.5 MPa H₂
13 pressure, for 24 h per run. For each run, the catalyst was separated by filtration from the reaction
14 mixture and reused in the follow up run. A total of six reaction cycles were carried out.
15
16
17
18

19 **Leaching tests**

20 Leaching tests were performed to check if any Pd dissolves in the reaction mixture and to
21 determine if a homogeneous reaction takes place. The procedure was the following: the catalyst
22 from the reaction mixture obtained after the first reaction cycle was filtered at RT and at high
23 temperature (hot filtration) using filter paper and the remaining filtrate was again pressurized
24 with H₂ and subjected to the reaction without catalyst. The results are displayed in Table S3,
25 entries 3 and 4, from which we conclude that no leaching of the catalyst occurred.
26
27
28
29
30

31 **Analysis of reaction products**

32 Separation and determination of the analytes was performed by gas chromatography (GC)
33 and a quadrupole mass spectrometer (MS) (Shimadzu GC-MS-QP2010 Ultra GC-MS)
34 equipped with a ShinCarbon ST Micropacked column (2 m x 1 mm, OD 1/16", mesh 100/120,
35 temperature limits up to 300 °C).
36
37
38
39

40 The GC conditions for the sample analysis were: Injector temperature: 275 °C; Carrier gas:
41 helium; Pressure: 120.0 kPa; Linear velocity: 52.9 cm/s; Oven temp.: 40 °C (hold 1 min.) to
42 50 °C at 2 °C min⁻¹, then to 200 °C at 40 °C min⁻¹ then to 280 °C at 15 °C min⁻¹ (hold 20 min).
43 Detector: MS (EI); Ion source temp.: 200 °C; Interface temp.: 250 °C; Detector voltage: 0.8
44 kV.
45
46
47

48 Activity results are expressed in terms of 4-NS conversion (moles reacted over the initial
49 number of moles) and selectivity to 4-AS (moles of 4-AS produced over the moles of reacted
50 4-NS). TOF represents the total number of moles transformed per mole of Pd per second.
51
52
53
54

55 **Characterization methods**

56 XPS measurements were performed using a Kratos Ultra DLD Setup spectrometer using
57 the Ka and Al-K α (1486.74 eV) radiation produced by an X-ray source operating at a total
58 power of 300 W (12.0 kV \times 25 mA) and a vacuum of $\approx 1 \times 10^{-4}$ MPa.
59
60

1
2
3 The H₂ temperature programmed desorption experiments (H₂-TPD) were performed using
4 a Porotec TPDRO 1100 device. Prior to the adsorption step, approximately 50 mg of sample
5 was pretreated for 1 h at 200 °C in a He gas flow to ensure a clean surface, after which it was
6 cooled down to RT also in a He gas flow. A 5 vol. % H₂-He mixture was passed over the sample
7 with a flow rate of 50 mL min⁻¹ for 1 h. This was followed by He gas passed for 10 minutes
8 through the sample to again clean the surface and the temperature was linearly increased by 10
9 °C min⁻¹ to 800 °C. The quantification of the H₂ released during desorption process was carried
10 out by using the equipped thermal conductivity detector of the TPDRO device and a calibration
11 curve.
12

13
14
15
16
17
18
19 The XRD measurements were performed using a Bruker-AXS D8 Advance diffractometer
20 equipped with a LynxEye 1D detector and Cu-Kα (0.1541 nm) radiation source and a
21 scintillation counter detector. The diffraction patterns were recorded at an 2θ angle in the range
22 of 9-90°, with a step size of 0.02° and a rate of 1.2° min⁻¹. For the identification of the XRD
23 phases present in the samples, the Powder Diffraction File from the International Centre for
24 Diffraction Data (PDF-ICDD) was used.
25

26
27
28
29 The FTIR spectra were acquired using a Perkin Elmer Spectrum BX II apparatus, equipped
30 with a Pike-MIRacle ATR attachment having a diamond/ZnSe crystal plate. The spectra were
31 recorded in attenuated total reflection (ATR) mode, with a resolution of 4 cm⁻¹. A total of 128
32 scans were collected. The investigated wavenumber domain was set in the range of 500-4000
33 cm⁻¹.
34

35
36
37 The Raman spectra were recorded in the range between 50 and 2000 cm⁻¹, using a HORIBA
38 Jobin-Yvon LabRAM HR evolution spectrometer equipped with an air cooled CCD and a He-
39 Ne laser with a wavelength of 633 nm. The spectra were recorded in the extended scan mode
40 with acquisition time of 5x60 s.
41

42
43
44 All TEM observations were been performed with a JEOL2100 system, equipped with X-
45 Ray spectrometer and ASTAR crystallographic tool developed by NANOME GAS.
46

47
48 A Perkin Elmer NexION 300S ICP Mass Spectrometer, MS, was used for the determination
49 of the Pd content. The instrument was equipped with Pt sampling and skimmer cones, a PFA
50 nebulizer, quartz spray chamber, quartz torch and PC3 Peltier Cooler inlet system. The
51 instrument also includes a hyper skimmer to focus the ion beam. The ICP-MS system was
52 operated using a collision cell with kinetic energy discrimination (KED), which utilizes He gas
53 flow (5.4 mL min⁻¹) for an effective removal of most common polyatomic interferences.
54 Samples were measured in triplicate. The analyte mass (m/z) - ¹⁰⁶Pd was acquired. The
55 equipment was calibrated in the range 0.05 – 4.00 μg L⁻¹ Pd. The reference material used for
56
57
58
59
60

1
2
3 calibration was a 1000 $\mu\text{g mL}^{-1}$ Pd pure single-element standard in 10% HCl, supplied by
4 Perkin Elmer. All glassware used for the analysis was cleaned with 5% HNO_3 solution and
5 rinsed with ultrapure water.
6
7
8
9

10 **AUTHOR INFORMATION**

11 **Corresponding Author**

12 *Email: mihaela.florea@infim.ro and barsoumw@drexel.edu
13
14
15

16 **ORCID**

17 Mihaela Trandafir: 0000-0001-9001-8738

18 Florentina Neatu: 0000-0002-7885-436X

19 Stefan Neatu: 0000-0002-2450-0291

20 Mihaela Florea: 0000-0002-6612-6090
21
22

23 **Author contributions**

24 F.N., M.W.B., and M.F. conceived the project. V.N. prepared the MAX phases, M.M.T.
25 prepared the materials containing Pd and performed the catalytic tests reactions and TPD
26 studies, A.K. performed the TEM experiments, I.M.C performed the FTIR and Raman
27 spectroscopies and interpretation, E.I.C. performed the ICP experiments, F. N., S.N. and
28 M.M.T. performed XPS and XRD analysis and analyzed the data. All the authors wrote the
29 paper. All authors read and approved the final version of paper.
30
31
32
33
34

35 SI include experimental procedures, characterization data, GC-MS chromatograms
36
37
38

39 **Notes**

40 The authors declare no competing financial interest.
41
42
43
44

45 **ACKNOWLEDGMENTS**

46 MWB and VN were funded by NSF (DMR 1740795). FN, MMT, SN, MF acknowledge
47 the funding from Ministry of Research and Innovation, CNCS-UEFISCDI, project number PN-
48 III-P1.1-TE-2016-2116 and Romanian Ministry of Research and Innovation through the Core
49 Program PN19-030101. This work was also supported by a grant of the Romanian National
50 Authority for Scientific Research and Innovation, CCCDI – UEFISCDI, project number
51 111/2019, ERANET-M.-CATALEAST-1, within PNCDI III.
52
53
54
55
56
57

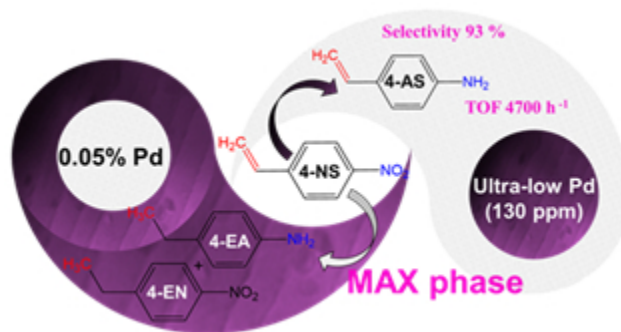
58 **REFERENCES**

59
60

1. Corma, A.; Serna, P.; Concepción, P.; Calvino, J. J., Transforming Nonselective into Chemoselective Metal Catalysts for the Hydrogenation of Substituted Nitroaromatics. *J. Am. Chem. Soc.* **2008**, *130* (27), 8748-8753.
2. Blaser, H.-U., A Golden Boost to an Old Reaction. *Science* **2006**, *313* (5785), 312.
3. Ono, N., *The nitro group in organic synthesis*. Wiley-VCH: New York, **2001**.
4. Blaser, H.-U.; Siegrist, U.; Steiner, H.; Studer, M., *Aromatic nitro compounds*. Wiley-VCH: Weinheim, **2001**.
5. Wei, H.; Liu, X.; Wang, A.; Zhang, L.; Qiao, B.; Yang, X.; Huang, Y.; Miao, S.; Liu, J.; Zhang, T., FeOx-Supported Platinum Single-Atom and Pseudo-Single-Atom Catalysts for Chemoselective Hydrogenation of Functionalized Nitroarenes. *Nat. Commun.* **2014**, *5*, 5634.
6. Corma, A.; Serna, P., Chemoselective Hydrogenation of Nitro Compounds with Supported Gold Catalysts. *Science* **2006**, *313* (5785), 332-334.
7. Boronat, M.; Concepción, P.; Corma, A.; González, S.; Illas, F.; Serna, P., A Molecular Mechanism for the Chemoselective Hydrogenation of Substituted Nitroaromatics with Nanoparticles of Gold on TiO₂ Catalysts: A Cooperative Effect between Gold and the Support. *J. Am. Chem. Soc.* **2007**, *129* (51), 16230-16237.
8. Serna, P.; Corma, A., Transforming Nano Metal Nonselective Particulates into Chemoselective Catalysts for Hydrogenation of Substituted Nitrobenzenes. *ACS Catal.* **2015**, *5* (12), 7114-7121.
9. Blaser, H.-U.; Steiner, H.; Studer, M., Selective Catalytic Hydrogenation of Functionalized Nitroarenes: An Update. *ChemCatChem* **2009**, *1* (2), 210-221.
10. Mao, J.; Chen, W.; Sun, W.; Chen, Z.; Pei, J.; He, D.; Lv, C.; Wang, D.; Li, Y., Rational Control of the Selectivity of a Ruthenium Catalyst for Hydrogenation of 4-Nitrostyrene by Strain Regulation. *Angewandte Chemie International Edition* **2017**, *56* (39), 11971-11975.
11. Carrus, M.; Fantauzzi, M.; Riboni, F.; Makosch, M.; Rossi, A.; Selli, E.; van Bokhoven, J. A., Increased Conversion and Selectivity of 4-Nitrostyrene Hydrogenation to 4-Aminostyrene on Pt Nanoparticles Supported on Titanium-Tungsten Mixed Oxides. *Appl. Catal. A* **2016**, *519*, 130-138.
12. Makosch, M.; Lin, W.-I.; Bumbálek, V.; Sá, J.; Medlin, J. W.; Hungerbühler, K.; van Bokhoven, J. A., Organic Thiol Modified Pt/TiO₂ Catalysts to Control Chemoselective Hydrogenation of Substituted Nitroarenes. *ACS Catal.* **2012**, *2* (10), 2079-2081.
13. Yang, N.; Cheng, H.; Liu, X.; Yun, Q.; Chen, Y.; Li, B.; Chen, B.; Zhang, Z.; Chen, X.; Lu, Q.; Huang, J.; Huang, Y.; Zong, Y.; Yang, Y.; Gu, L.; Zhang, H., Amorphous/Crystalline Hetero-Phase Pd Nanosheets: One-Pot Synthesis and Highly Selective Hydrogenation Reaction. *Adv. Mater.* **2018**, *30* (39), 1803234.
14. Barsoum, M. W.; El-Raghy, T., Synthesis and Characterization of a Remarkable Ceramic: Ti₃SiC₂. *J. Am. Ceram. Soc.* **1996**, *79* (7), 1953-1956.
15. Barsoum, M. W., *MAX Phases: Properties of machinable ternary carbides and nitrides*. Wiley-VCH Verlag GmbH & Co. KGaA: Weinheim, **2013**.
16. Barsoum, M. W.; Brodtkin, D.; El-Raghy, T., Layered Machinable Ceramics for High Temperature Applications. *Scripta Mater.* **1997**, *36* (5), 535-541.
17. Nowotny, V. H., Strukturchemie einiger Verbindungen der Übergangsmetalle mit den Elementen C, Si, Ge, Sn. *Prog. Solid State Chem.* **1971**, *5*, 27-70.
18. Sokol, M.; Natu, V.; Kota, S.; Barsoum, M. W., On the Chemical Diversity of the MAX Phases. *Trends Chem.* **2019**, *1* (2), 210-223.
19. Ng, W. H. K.; Gnanakumar, E. S.; Batyrev, E.; Sharma, S. K.; Pujari, P. K.; Greer, H. F.; Zhou, W.; Sakidja, R.; Rothenberg, G.; Barsoum, M. W.; Shiju, N. R., The Ti₃AlC₂ MAX Phase as an Efficient Catalyst for Oxidative Dehydrogenation of n-Butane. *Angew. Chem. Int. Ed.* **2017**, *57* (6), 1485-1490.

- 1
2
3 20. Primo, A.; Neatu, F.; Florea, M.; Parvulescu, V.; Garcia, H., Graphenes in the Absence of
4 Metals as Carbocatalysts for Selective Acetylene Hydrogenation and Alkene Hydrogenation.
5 *Nat Commun* **2014**, *5*, 5291.
- 6 21. Holschumacher, D.; Bannenberg, T.; Hrib Cristian, G.; Jones Peter, G.; Tamm, M.,
7 Heterolytic Dihydrogen Activation by a Frustrated Carbene–Borane Lewis Pair. *Angew. Chem.*
8 *Int. Ed.* **2008**, *47* (39), 7428-7432.
- 9 22. Mitsudome, T.; Mikami, Y.; Matoba, M.; Mizugaki, T.; Jitsukawa, K.; Kaneda, K., Design
10 of a Silver–Cerium Dioxide Core–Shell Nanocomposite Catalyst for Chemoselective
11 Reduction Reactions. *Angew. Chem. Int. Ed.* **2012**, *51* (1), 136-139.
- 12 23. Corma, A.; Garcia, H.; Leyva, A., Catalytic Activity of Palladium Supported on Single
13 Wall Carbon Nanotubes Compared to Palladium Supported on Activated Carbon: Study of the
14 Heck and Suzuki Couplings, Aerobic Alcohol Oxidation and Selective Hydrogenation. *J. Mol.*
15 *Catal. A-Chem.* **2005**, *230* (1–2), 97-105.
- 16 24. Davies, I. W.; Matty, L.; Hughes, D. L.; Reider, P. J., Are Heterogeneous Catalysts
17 Precursors to Homogeneous Catalysts? *J. Am. Ceram. Soc.* **2001**, *123* (41), 10139-10140.
- 18 25. García-Mota, M.; Gómez-Díaz, J.; Novell-Leruth, G.; Vargas-Fuentes, C.; Bellarosa, L.;
19 Bridier, B.; Pérez-Ramírez, J.; López, N., A Density Functional Theory Study of the ‘Mythic’
20 Lindlar Hydrogenation Catalyst. *Theor. Chem. Acc.* **2011**, *128* (4), 663-673.
- 21 26. Ulan, J. G.; Kuo, E.; Maier, W. F.; Rai, R. S.; Thomas, G., Effect of Lead Acetate in the
22 Preparation of the Lindlar Catalyst. *J. Org. Chem.* **1987**, *52* (14), 3126-3132.
- 23 27. Lin, F.; Hoang, D. T.; Tsung, C.-K.; Huang, W.; Lo, S. H.-Y.; Wood, J. B.; Wang, H.;
24 Tang, J.; Yang, P., Catalytic Properties of Pt Cluster-Decorated CeO₂ Nanostructures. *Nano*
25 *Res.* **2011**, *4* (1), 61-71.
- 26 28. Liu, W.; Jiang, Y.; Dostert, K.-H.; O’Brien, C. P.; Riedel, W.; Savara, A.; Schauermaann,
27 S.; Tkatchenko, A., Catalysis Beyond Frontier Molecular Orbitals: Selectivity in Partial
28 Hydrogenation of Multi-Unsaturated Hydrocarbons On Metal Catalysts. *Sci. Adv.* **2017**, *3* (7),
29 e1700939.
- 30 29. Bridier, B.; López, N.; Pérez-Ramírez, J., Molecular Understanding of Alkyne
31 Hydrogenation for the Design of Selective Catalysts. *Dalton Trans.* **2010**, *39* (36), 8412-8419.
- 32 30. Segura, Y.; López, N.; Pérez-Ramírez, J., Origin of the Superior Hydrogenation Selectivity
33 of Gold Nanoparticles in Alkyne + Alkene Mixtures: Triple- Versus Double-Bond Activation.
34 *J. Catal.* **2007**, *247* (2), 383-386.
- 35 31. Wang, L.; Zhang, J.; Wang, H.; Shao, Y.; Liu, X.; Wang, Y.-Q.; Lewis, J. P.; Xiao, F.-S.,
36 Activity and Selectivity in Nitroarene Hydrogenation over Au Nanoparticles on the
37 Edge/Corner of Anatase. *ACS Catal.* **2016**, *6* (7), 4110-4116.
- 38 32. Ding, Y.; Li, X.; Pan, H.; Wu, P., Ru Nanoparticles Entrapped in Ordered Mesoporous
39 Carbons: An Efficient and Reusable Catalyst for Liquid-Phase Hydrogenation. *Catal. Letters*
40 **2014**, *144* (2), 268-277.
- 41 33. Sreedhar, B.; Rawat, V. S., Mild and Efficient PtO₂-Catalyzed One-Pot Reductive Mono-
42 N-alkylation of Nitroarenes. *Synth. Commun.* **2012**, *42* (17), 2490-2502.
- 43 34. Jiang, F.; Cai, J.; Liu, B.; Xu, Y.; Liu, X., Particle Size Effects in the Selective
44 Hydrogenation of Cinnamaldehyde Over Supported Palladium Catalysts. *RSC Adv.* **2016**, *6*
45 (79), 75541-75551.
- 46 35. Nagendiran, A.; Pascanu, V.; Bermejo Gómez, A.; González-Miera, G.; Tai, C.-W.; Verho,
47 O.; Martín-Matute, B.; Bäckvall, J.-E., Mild and Selective Catalytic Hydrogenation of the C=C
48 Bond in α,β -Unsaturated Carbonyl Compounds Using Supported Palladium Nanoparticles.
49 *Chem. Eur. J.* **2016**, *22* (21), 7184-7189.
- 50 36. Mehrabadi, B. A. T.; Eskandari, S.; Khan, U.; White, R. D.; Regalbuto, J. R., Chapter One
51 - A Review of Preparation Methods for Supported Metal Catalysts. In *Advances in Catalysis*,
52 Song, C., Ed. Academic Press: **2017**; Vol. 61, pp 1-35.
- 53
54
55
56
57
58
59
60

- 1
2
3 37. Zhang, L.; Zhou, M.; Wang, A.; Zhang, T., Selective Hydrogenation over Supported Metal
4 Catalysts: From Nanoparticles to Single Atoms. *Chem. Rev.* **2020**, *120* (2), 683-733.
5
6 38. Trandafir, M. M.; Pop, L.; Hadade, N. D.; Florea, M.; Neatu, F.; Teodorescu, C. M.; Duraki,
7 B.; van Bokhoven, J. A.; Grosu, I.; Parvulescu, V. I.; Garcia, H., An Adamantane-Based COF:
8 Stability, Adsorption Capability, and Behaviour as a Catalyst and Support for Pd and Au for
9 the Hydrogenation of Nitrostyrene. *Catal. Sci. Technol.* **2016**, *6* (23), 8344-8354.
10
11 39. Lu, J.; Aydin, C.; Browning, N. D.; Gates, B. C., Hydrogen Activation and Metal Hydride
12 Formation Trigger Cluster Formation from Supported Iridium Complexes. *J. Am. Chem. Soc.*
13 **2012**, *134* (11), 5022-5025.
14
15 40. Vilé, G.; Albani, D.; Nachtegaal, M.; Chen, Z.; Dontsova, D.; Antonietti, M.; López, N.;
16 Pérez-Ramírez, J., A Stable Single-Site Palladium Catalyst for Hydrogenations. *Angew. Chem.*
17 *Int. Ed.* **2015**, *54* (38), 11265-11269.
18
19 41. Amer, M.; Barsoum, M. W.; El-Raghy, T.; Weiss, I.; Leclair, S.; Liptak, D., The Raman
20 Spectrum of Ti_3SiC_2 . *J. Appl. Phys.* **1998**, *84* (10), 5817-5819.
21
22 42. Beran, A.; Libowitzky, E., Spectroscopic Methods in Mineralogy. Mineralogical Society
23 of Great Britain and Ireland: 2004.
24
25 43. Barsoum, M. W.; El-Raghy, T.; Ogbuji, L. U. J. T., Oxidation Of Ti_3SiC_2 in Air. *J.*
26 *Electrochem. Soc.* **1997**, *144* (7), 2508-2516.
27
28
29
30
31
32
33
34
35
36
37
38
39
40
41
42
43
44
45
46
47
48
49
50
51
52
53
54
55
56
57
58
59
60



83x44mm (96 x 96 DPI)

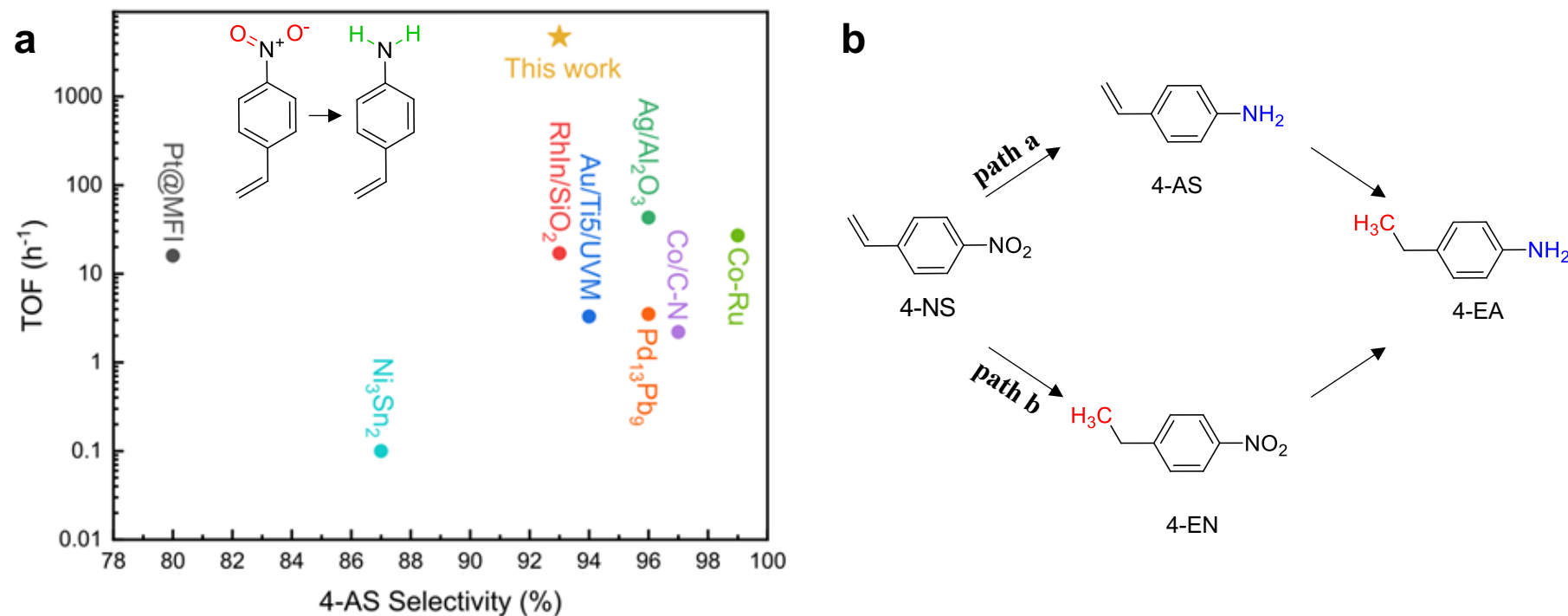
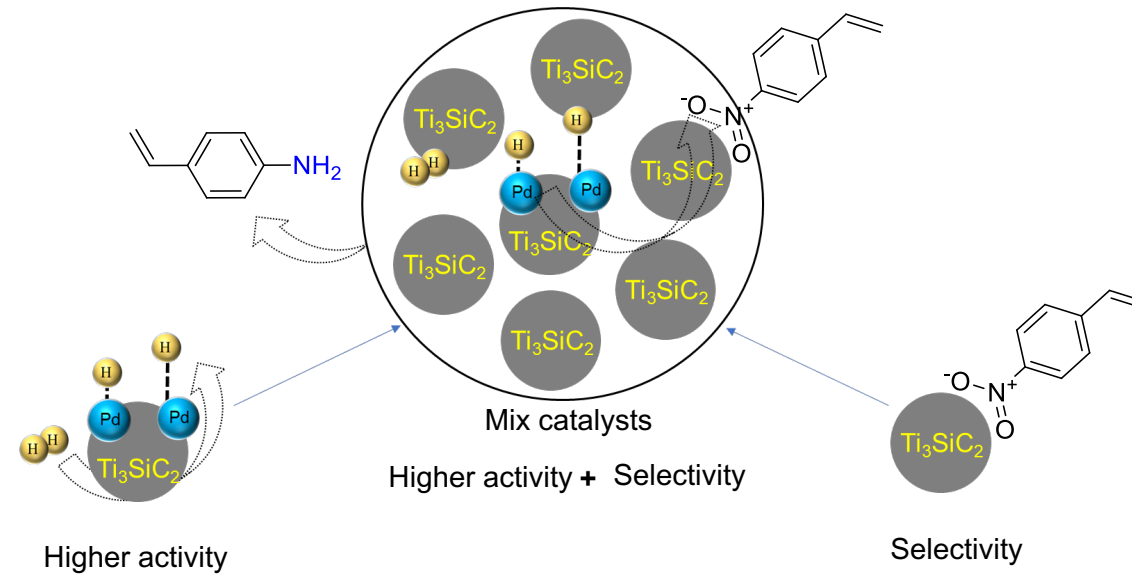


Figure 1: a) Semi-log plot of our TOF results compared with some of the highest reported in the literature for catalysts with 100% conversion and > 80% selectivities of 4-NS to 4-AS. Left top inset shows 4-NS molecule; top right inset shows desired molecule, 4-AS. b) Reaction pathways for hydrogenation of 4-NS.



Scheme 1. Schematic of mechanical mixture preparation and its benefits.